

**Proof Delivery Form**  
**Please return this form with your proof**

**CUP reference:**

**Date of delivery:**

**Journal and Article number:** MAP 239

**Volume and Issue Number:** 13(4)

**Number of colour figures:** Nil

**Number of pages (not including this page):** 14

---

**Meteorological Applications**

Here is a proof of your article for publication in the Journal. Please print out the file and check the proofs carefully, make any corrections necessary on a hardcopy, and answer queries on the proofs. Any figures which are in colour are in the file – they should be viewed on screen. If there are any problems with colour illustrations please email me as below.

Please return the **corrected hardcopy proof** together with the **offprint order form** as soon as possible (no later than 4 days after receipt) to:

Carol Miller  
Journal Office  
Cambridge University Press  
The Edinburgh Building  
Shaftesbury Road  
Cambridge  
CB2 2RU

To avoid delay from overseas, please send the proof by air mail or courier.

- You are responsible for correcting your proofs. Errors not found may appear in the published journal.
- The proof is sent to you for correction of typographical errors only. Revision of the substance of the text is not permitted, unless discussed with the editor of the journal.
- Please answer carefully any queries raised from the typesetter.
- A new copy of a figure must be provided if correction of anything other than a typographical error introduced by the typesetter is required.
- If the paper was written in LateX, please do not send corrections as Latex code, we have now translated the Latex to typesetting code.

If you have no corrections to make please contact [cmiller@cambridge.org](mailto:cmiller@cambridge.org) to save having to return your paper proof.

Corrections can be sent on email if they are light – please quote page number and line number.

---

**Author queries:**

Q1: Single author in ref. list.

---

**Typesetter queries:**

---

**Non-printed material:**

# Offprint order form



**CAMBRIDGE**  
UNIVERSITY PRESS

PLEASE COMPLETE AND RETURN THIS FORM. WE WILL BE UNABLE TO SEND OFFPRINTS (INCLUDING FREE OFFPRINTS) UNLESS A RETURN ADDRESS AND ARTICLE DETAILS ARE PROVIDED.

VAT REG NO. GB 823 8476 09

## Meteorological Applications (MAP)

Volume:  no:

### Offprints

50 offprints of each article will be supplied free to each **first named author and sent to a single address**. Please complete this form and send it to **the publisher (address below)**. Please give the address to which your offprints should be sent. They will be despatched by surface mail within one month of publication. For an article by **more than one author this form is sent to you as the first named**. **All extra offprints should be ordered by you in consultation with your co-authors.**

Number of offprints required in addition to the 50 free copies:

Email: .....

Offprints to be sent to (print in **BLOCK CAPITALS**): .....

.....

.....

Post/Zip Code: .....

Telephone: ..... Date (dd/mm/yy): ..... / ..... / .....

Author(s): .....

.....

Article Title: .....

.....

All enquiries about offprints should be addressed to **the publisher**: Journals Production Department, Cambridge University Press, The Edinburgh Building, Shaftesbury Road, Cambridge CB2 2RU, UK.

### Charges for extra offprints (excluding VAT) Please circle the appropriate charge:

Number of copies	25	50	100	150	200	per 50 extra
1-4 pages	£68	£109	£174	£239	£309	£68
5-8 pages	£109	£163	£239	£321	£399	£109
9-16 pages	£120	£181	£285	£381	£494	£120
17-24 pages	£131	£201	£331	£451	£599	£131
Each Additional 1-8 pages	£20	£31	£50	£70	£104	£20

### Methods of payment

If you live in Belgium, France, Germany, Ireland, Italy, Portugal, Spain or Sweden and are not registered for VAT we are required to charge VAT at the rate applicable in your country of residence. If you live in any other country in the EU and are not registered for VAT you will be charged VAT at the UK rate.

If registered, please quote your VAT number, or the VAT number of any agency paying on your behalf if it is registered. VAT Number: .....

Payment **must** be included with your order, please tick which method you are using:

- Cheques should be made out to Cambridge University Press.
- Payment by someone else. Please enclose the official order when returning this form and ensure that when the order is sent it mentions the name of the journal and the article title.
- Payment may be made by any credit card bearing the Interbank Symbol.

Card Number:

Expiry Date (mm/yy): ..... / ..... Card Verification Number:

The card verification number is a 3 digit number printed on the **back** of your **Visa** or **Master card**, it appears after and to the right of your card number. For **American Express** the verification number is 4 digits, and printed on the **front** of your card, after and to the right of your card number.

Signature of card holder: ..... Amount (Including VAT if appropriate): £ .....

Please advise if address registered with card company is different from above

# The influence of synoptic-mesoscale winds and sea surface temperature distribution on fog formation near the Korean western peninsula

Hyo Choi<sup>1</sup> & Milton S. Speer<sup>2</sup>

<sup>1</sup>Department of Atmospheric Environmental Sciences, Kangnung National University, Kangnung, Kangwondo, 210-702, Korea

Email: du8392@hanmail.net

<sup>2</sup>School of Mathematics and Statistics, The University of New South Wales, Sydney, Australia

*When high pressure is located near the Korean peninsula, a diffluent wind regime generally occurs over the Yellow Sea. At night or early morning, diffluent westerly winds occur on the western side of the Korean peninsula near Incheon city and encounter a combined land breeze and katabatic easterly offshore wind, resulting in conditions ranging from calm to a moderate westerly wind near the coast. Nocturnal radiational cooling of the land surface and the moisture laden westerly winds can cause air near the coast to become saturated, resulting in coastal advection fog. During the day, on the other hand, the synoptic-scale westerly wind is reinforced by a westerly sea breeze and is further reinforced by a westerly valley wind directed upslope towards the mountain top. Even if the resulting intensified onshore wind could transport a large amount of moisture from the sea over the land, it would be very difficult for fog to form because the daytime heat flux from the ground would develop the convective boundary layer inland from Incheon city sufficiently to reduce significantly the moisture content of the air. Therefore, fog does not generally form in situ over the inland coastal basin. When an area of cold sea water (10 °C average) exists approximately 25–50 km offshore and the sea surface temperature increases towards the coast, air parcels over the cool sea surface are cooled sufficiently to saturation, resulting in the formation of advection sea fog. However, at the coast, nocturnal cooling of the ground further cools the advected moist air driven by the westerly wind and causes coastal advection fog to form.*

**Keywords:** diffluent westerly wind, Yellow Sea, Incheon, Seoul, sea-surface temperature, advection fog, sea-land breeze, valley-katabatic wind

Received 9 January 2006, revised 14 August 2006

## 1. Introduction

Although several numerical modelling experiments have investigated the formation of Yellow Sea fog or fog over the Korean western peninsula, improvements in fog forecasting accuracy are difficult to achieve. Sciocatti (1984) demonstrated the effect of sea-surface temperature (SST) on the formation/dispersal of advection fog with the passage of a coastal low pressure system. The coastal low usually accompanies a frontal system, which is generated by the effect of contrasting air mass properties, and synoptic-scale fog results over the open sea or over a wide area of the coast. Won et al. (2000) analysed meteorological and oceanographic characteristics on the formation of sea fog over the Yellow Sea, and Lee et al. (2000) explained turbulent effects associated with the fog. Ahn et al. (2002) developed a sea-fog forecasting module and applied it to Ulung Island sea-fog events over the East Sea adjacent

to Korea. These three studies are based on a synoptic-scale approach focusing on the open sea and do not explain the formation of coastal fog or local-scale sea fog next to the coast caused by orographic effects in the coastal boundary layer. Even in the absence of a coastal low, there are frequent occurrences of sea fog and coastal fog over the Yellow Sea (KMA, 1997). The accumulation or dissipation of heat over the sea and the inland coastal basin are very important factors in fog formation (Raynor et al. 1979, Whiteman 1990).

Fog formation over the open sea depends mainly upon humidity, which is a function of the temperature difference between the sea surface and boundary layer air above. Also, salt nuclei in the marine boundary layer can readily lead to the formation of water droplets below 80% relative humidity, which can enhance fog formation in the coastal region. However, it is difficult to explain the driving mechanism for the formation of

Q1



**Figure 1.** Topographical features near Seoul in the fine-mesh model domain. 'S' denotes the Seoul metropolitan area and 'In' denotes Incheon city. The study area is located in the western coastal region of the Korean peninsula, and consists of the Yellow Sea in the west, a low dune area in the central part and a mountainous area in the east.

coastal fog due to the complexity of processes involved (Choi et al. 1998). Recently, enhancements of NOAA and GMS satellite imagery have been used to detect fog, but they provide only current information on fog formation. Distinguishing low cloud from fog over areas larger than about 20 km<sup>2</sup> is possible now with the use of satellite imagery. Numerical model output, including temperature, moisture and wind fields, provides useful predictive information for fog and its generating mechanisms. However, accurate prediction of fog in the complex coastal terrain of the Korean peninsula remains problematic. Near the Korean peninsula, the formation of coastal fog is not only affected directly by the air-sea temperature difference, but also by both sea-land breezes and mountain-valley winds which are driven by thermal contrasts over the coast and mountain terrain (Choi 1996, Choi et al. 2000).

In this study, through a comparison of observed data with the results of predicted numerical model variables and derived fields critical for fog formation, a mechanism for the formation of sea and coastal fog along the Yellow Sea coast of Korea is described.

## 2. Description of study area

The study area includes the Yellow Sea coast of Korea and surrounding terrain covering a total area approximately 250 km × 250 km (Figure 1). Incheon is a coastal city approximately 50 km south of Seoul, located on low dunes less than 100 m in height that extend 10 km inland from the coast and which are bordered by low mountains further inland. Seoul occupies an inland basin surrounded by mountains higher than 400 m in parts.

Further inland from the basin, Mt Yongmoon is much higher, at 1150 m as shown in Figure 4a in the fine-mesh model domain. Thus, the climate near Incheon city is generally affected by the temperature and moisture contrast produced by both sea and mountains from the resulting diurnal and nocturnal wind fields.

## 3. Model description

A three-dimensional non-hydrostatic grid point model using a terrain-following coordinate system ( $x, y, z^*$ ), called LAS-V was adapted for this study. LAS-V was originally developed at the Meteorological Research Institute (MRI), Japan Meteorological Agency (JMA), to investigate not only the large scale atmospheric circulation over north eastern Asia and local scale circulations in the mountainous coastal regions, including Korea, but also the atmospheric boundary layer (Takahashi 1998). The LAS-V model consists of three-dimensional hydrostatic and non-hydrostatic options in a terrain following coordinate system ( $x, y, z^*$ ) based upon Boussinesq and anelastic approximations. Time integration uses the Euler-backward scheme (in this study  $\Delta t = 30$  s, coarse-mesh;  $\Delta t = 10$  s, fine-mesh) and for integration in the vertical  $z$ -coordinate the Crank-Nicholson scheme is adopted. The radiative transfer condition of Klemp & Durran (1983) is applied to the atmospheric pressure changes at the model top boundary. The periodic lateral boundary condition of Orlanski (1976) is applied to the calculation of  $u, v$ , potential temperature and specific humidity. In the surface boundary layer, vertical diffusion coefficients for momentum and heat are evaluated from a turbulent closure level-2 model (Yamada 1983, Yamada & Mellor 1983). The simplified scheme of Katayama (1972) for computing radiative transfer in the troposphere is used to evaluate total net flux of long wave radiation absorbed by both H<sub>2</sub>O and CO<sub>2</sub>. The vertical flux from the ground was taken to have a positive sign, and incorporates H<sub>2</sub>O and CO<sub>2</sub> transmission functions, effective vapour amount, specific humidity and pressure. Similarity theory is adopted for the energy budget near the surface, and the surface boundary layer is assumed to be a constant flux layer in order to estimate sensible and latent heat fluxes (Businger 1973, Monin 1970). The force restore method of Deardorff (1978) was used to calculate the diurnal variation of soil temperature and specific humidity at the surface. Full model details including the numerics, radiative transfer and boundary layer schemes are available in Kimura & Arakawa (1983), Kimura & Takahashi (1991), Takahashi (1998) and Choi et al. (2004).

The numerical simulations in this study were performed on a Hitachi super computer at MRI. One-way double nesting was employed with two domains (coarse-mesh and fine-mesh) each consisting of 50 × 50 grid points. A uniform horizontal interval of 20 km was used for the coarse-mesh model domain, and 5 km for the

fine-mesh domain. In both domains, 16 vertical levels from a height of 10 m above ground level to 6 km (the top of the model domain) were used with sequentially larger intervals with height. The 12-h JMA gridded global analysis data (G-ANAL), at a horizontal resolution of  $1.25^\circ$ , including atmospheric pressure, wind, potential temperature and specific humidity at five levels between the surface and 100 hPa (approximately 13 km), were horizontally and vertically interpolated to the 16 levels of the coarse-mesh domain. The coarse-mesh model fields were treated as lateral boundary conditions for the fine-mesh domain. SST fields that were used as initial input data in both the coarse-mesh and fine-mesh model domains were derived from GMS and NOAA satellite imagery by a reanalysis technique developed by the National Fisheries Research and Development Agency of Korea (NFRDA 1998).

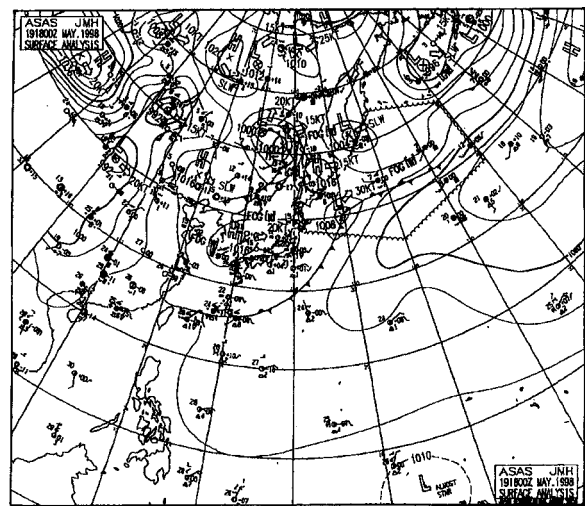
## 4. Results and discussion

### 4.1. Fog formation (early morning)

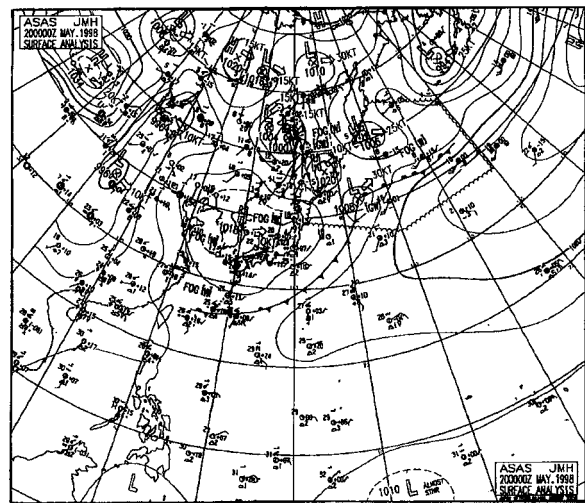
LAS-V was initialised at 1200 UTC 19 May, 1998 (2100 LST 19 May) and the first 12 hours were used as model spin-up time to ensure stable boundary conditions. In order to verify the formation of coastal fog near Incheon Bay and to investigate the driving mechanism for its development over one full 24-h period, only the simulation results from 0600 LST 20 May to 0600 LST 21 May, are illustrated here.

On the SLP chart at 1800 UTC, 19 May (0300 LST, May 20), 1998 (Figure 2a), high pressure is centred over the south-eastern part of the Korean peninsula, and a synoptic-scale southwesterly wind prevails near Incheon city on the central part of the Korean west coast. At 0000 UTC, 20 May (0900 LST), even when the high pressure centre has moved to the East Sea on the eastern side of the Korean peninsula, the synoptic-scale southwesterly wind still prevails near Incheon city (Figures 2b and 3b). At 1800 UTC 19 May (0300 LST, May 20), sea fog was reported near the southern part of the Yellow Sea on the JMA mean sea level pressure (SLP) chart. Incheon Meteorological Observatory reported the formation of fog with a relative humidity of 96%. The non-hydrostatic numerical simulation results containing Incheon city in the fine-mesh domain indicates a relative humidity of 92% and hence the likelihood of fog formation.

To understand the driving mechanism for the fog formation, it is necessary to analyse the possibility of both moisture advection and cooling of air parcels to saturation in the fog area. For moisture advection the wind fields were analysed on the synoptic and mesoscale. In the coarse-mesh domain, as shown in Figure 3a, diffluence occurs around the central part of the Yellow Sea and the wind speed increases away from the centre. Even though the synoptic-scale



2a

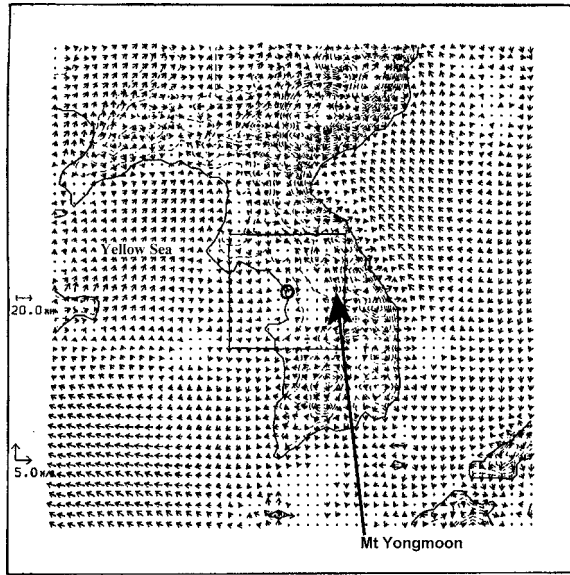


2b

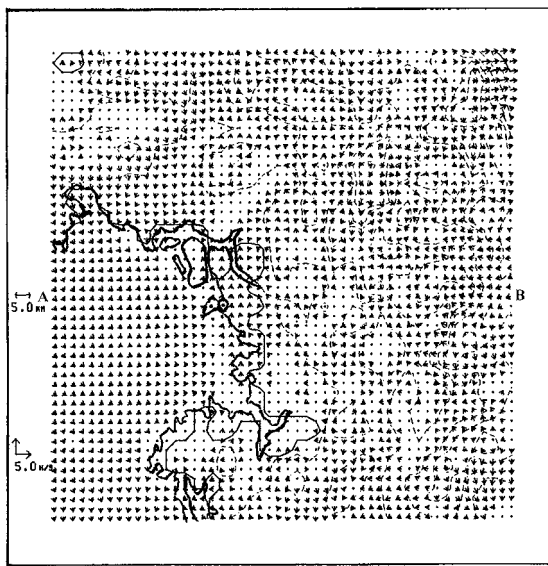
**Figure 2.** (a) MSLP chart centred over the Korean peninsula at 1800 UTC, 19 May 1998 (0300 LST, 20 May); (b) as for (a) except at 0000 UTC, 20 May (0900 LST, 21 May). High pressure is centred over the Korean peninsula (Japan in the centre of chart) and a synoptic-scale southwesterly wind prevails near Incheon city over the central part of the Korean west coast.

southwesterly wind is directed from the sea towards the Korean peninsula, the local wind pattern does not directly correspond to the synoptic-scale wind pattern. A diffluent northwesterly wind extends toward the central inland side of the Korean western peninsula near Incheon city where it meets an easterly wind that consists of a combined land breeze and mountain or katabatic wind, and results in a calm zone at the coast and inland. At this time (0600 LST, 20 May), the model wind speed closely matches the observed wind speed at Incheon Meteorological Observatory. In the fine-mesh domain (Figure 3b), the wind speed at Incheon is similar to the observed wind speed.

With regard to moisture advection, the vertical wind profile ( $\text{m s}^{-1}$ ) on a line A to B in Figure 3b is shown in Figures 4a and 4b. A synoptic-scale westerly wind of



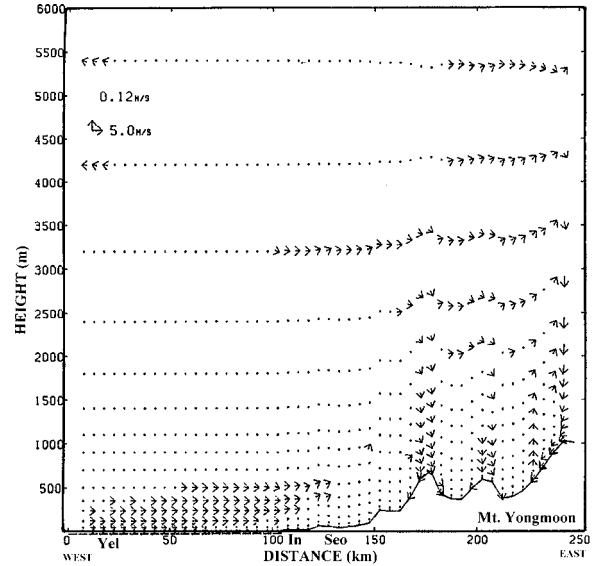
3a (revised)



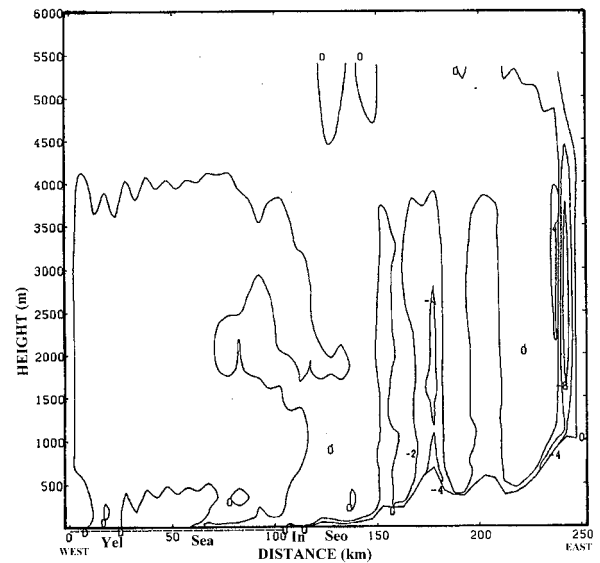
3b

**Figure 3.** Wind vector field ( $m s^{-1}$ ) at 0600 LST, 20 May, 1998 (+12 h) in (a) the coarse-mesh domain near the Korean peninsula; and (b), as for (a), except for the fine-mesh domain near Inchon city. The square and small circle symbols and the lines (dashed) denote the fine-mesh domain, Inchon city and topographical contours, respectively. Note the diffluent wind field in the centre of the Yellow Sea. The synoptic-scale westerly wind meets an easterly land breeze just off the coast near Inchon city, resulting in a calm zone.

$2.5 m s^{-1}$  is directed from the Yellow Sea towards the coast and becomes calm in the coastal region because of an opposing mountain or katabatic wind of  $2.5 m s^{-1}$  directed from the top of the mountains further inland. This also combines with a land breeze directed from the inland plain near Inchon city toward the Yellow Sea, thereby suppressing the synoptic-scale westerly wind and results in the calm zone. Essentially, moisture advection from the Yellow Sea towards the Inchon coast takes place with the synoptic-scale westerly wind and the moisture can be transported further inland by



4a

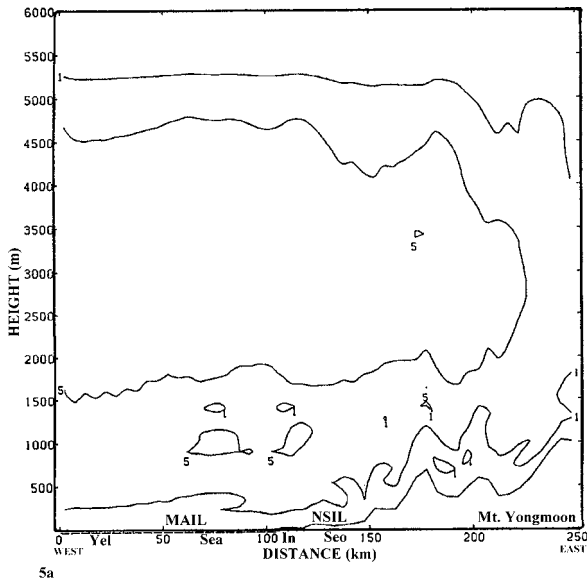


4b

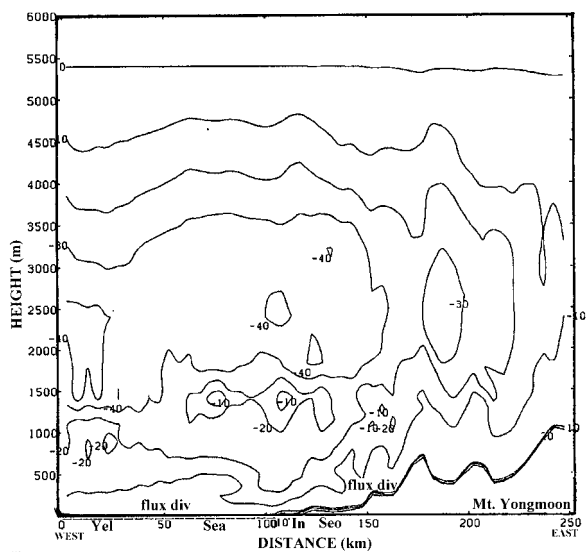
**Figure 4.** (a) Vertical wind profile ( $m s^{-1}$ ; horizontal scale and  $cm s^{-1}$ ; vertical scale) on a line AB (Yellow Sea–Inchon–Mt Yongmoon) in Figure 3b; and (b) as for (a) except for vertical wind speed ( $cm s^{-1}$ ). The synoptic-scale westerly wind meets a combined easterly katabatic land breeze and a calm zone is evident over a wide area of the coast and adjacent sea near Inchon and Seoul. ‘Yel’, ‘Sea’, ‘In’ and ‘Seo’ denote the Yellow Sea, coastal sea, Inchon city and Seoul city, respectively. Positive values of vertical wind speed ( $cm s^{-1}$ ) imply upward vertical motion.

a diurnal westerly sea breeze before sunset. By 0600 LST the next morning, radiational cooling should be sufficient to cause the moisture to condense into fog under a calm wind regime (Figures 5a, 5b, 6a and 6b).

Further analysis of the nocturnal cooling and boundary layer structure as revealed in Figures 5a and 5b is now given. In Figure 5a, the vertical diffusion coefficient of turbulent heat ( $K_h$ ) can be easily adapted to estimate vertical motion arising from diurnal and nocturnal heat processes. A small vertical turbulent diffusion



5a

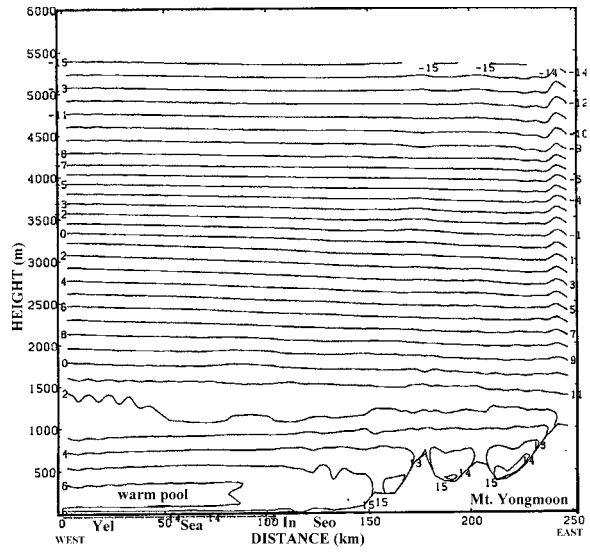


5b

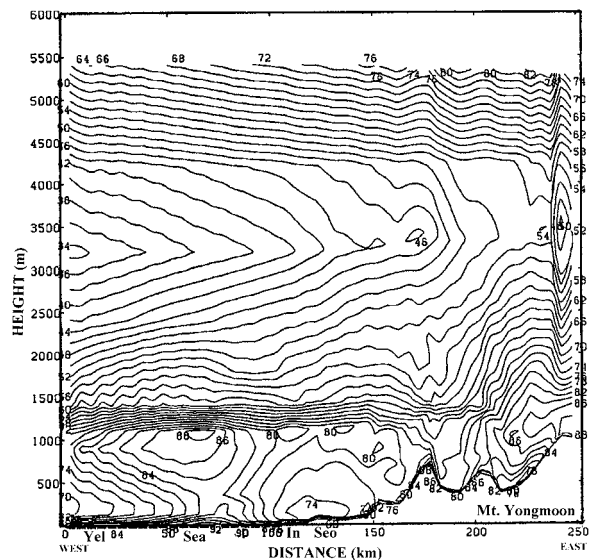
**Figure 5.** (a) As for Figure 4a, except for vertical profile of turbulent diffusion coefficient of turbulent heat ( $\text{m}^2 \text{s}^{-1}$ ); and (b) sensible heat flux ( $\text{W m}^{-2}$ ). NSIL and MAIL denote nocturnal surface inversion layer over the land surface at night and marine atmospheric inversion layer over the Yellow Sea. These two layers develop due to the greater air temperature over the sea surface ( $14^\circ\text{C}$ ) compared to the actual SST ( $10^\circ\text{C}$ ). 'Flux div' denotes divergence of sensible heat flux, which results in cooling of marine air and the formation of fog over the Yellow Sea, the coast and the inland basin near Incheon.

coefficient of heat ( $1.0 \text{ m}^2 \text{ s}^{-1}$ ) exists near the surface and indicates the occurrence of a thin, shallow, nocturnal surface inversion layer (NSIL) with a thickness of about 300 m. Its thickness increases higher in the mountains.

In Figure 5a, adiabatic warming is produced by the downward motion of air from the mountain top to the valley. This retards the cooling of air near the ground in the valley, resulting in a thicker NSIL on the mountain than near the coast. On the other hand, a marine atmospheric inversion layer (MAIL) forms to a thickness of about 250 m over the sea surface. The



6a

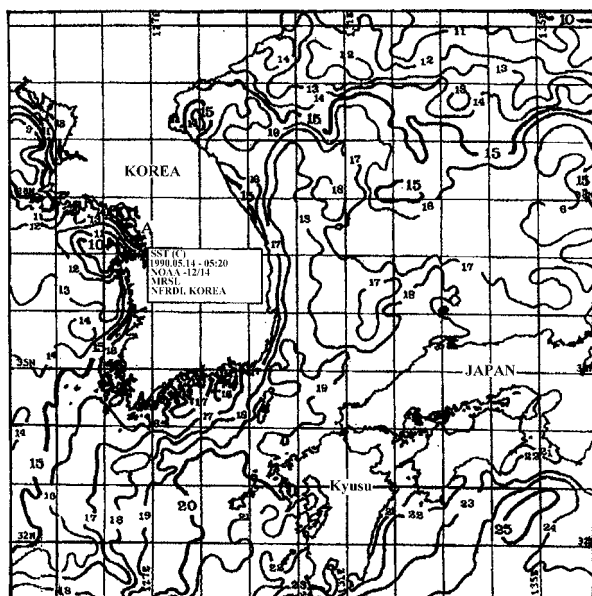


6b

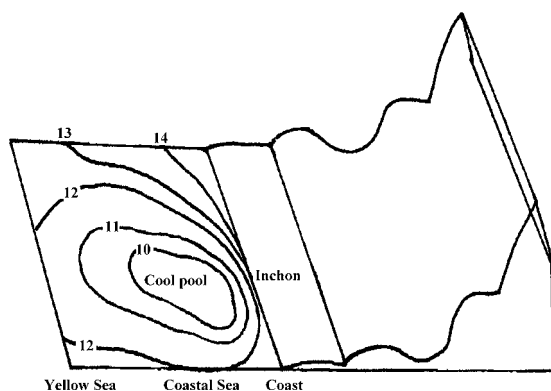
**Figure 6.** (a) As for Figure 5 except for vertical temperature profile ( $^\circ\text{C}$ ) over the Yellow sea (Yel), coastal sea (sea) and inland plain (In, Seo); and (b) as for (a) except for relative humidity (%). Note the warm pool over the Yellow Sea and NSIL over the inland surface. Relative humidity has a maximum value at a distance of about 25–50 km offshore, where cooling of air parcels occurs over SSTs of  $10^\circ\text{C}$ . Cloud forms with a base height about 1000 m above the sea surface, but no fog forms near Seoul over the surrounding inland basin.

thickness of the MAIL is slightly greater than the coastal NSIL of approximately 200 m because the cooling effect of the sea surface is smaller than that of the land surface.

Analysis of the cooling rate of air reveals that the sensible heat flux at the ground over the mountain surface and the coastal plain is  $+10 \text{ W m}^{-2}$  and the heat flux in the lower troposphere over the ground is  $-20 \text{ W m}^{-2}$  (Figure 5b). The vertical distribution of sensible heat flux produces sensible heat flux divergence, indicating that there is a loss in heat at the surface and cooling of air near the ground. However, sensible heat flux divergence over the Yellow Sea, including adjacent to the coast, is very small



7a



7b

**Figure 7.** (a) NOAA derived SST field ( $^{\circ}\text{C}$ ) on 20 May 1998 near the Korean peninsula; and (b) schematic profile of SST ( $^{\circ}\text{C}$ ) near the coast adjacent to Incheon. An area of minimum SST ( $10^{\circ}\text{C}$ ) is evident 25–70 km offshore. However, SST values nearer the coast reach as high as  $14^{\circ}\text{C}$ .

(between zero and  $-10 \text{ W m}^{-2}$ ) compared to over the inland coastal plain and the mountains (between  $+10$  and  $+20 \text{ W m}^{-2}$ ).

Over the coastal plain and adjacent sea and in the lower troposphere, small flux divergence occurs. This means that sensible heat flux divergence is greater at the top of the mountain than over the surface of the sea. Generally, it appears that the mountain surface cools more than the sea surface, and the air temperature of  $14^{\circ}\text{C}$  near the sea surface at night is little changed from that during the day. However, careful analysis of the sea-surface temperature distribution is needed because adjacent to the coast its distribution is complex, as shown in Figures 7a and 7b.

SSTs are as low as  $10^{\circ}\text{C}$  at approximately 25–50 km from the coast (Figures 7a and 7b) and the air temperature adjacent to the sea surface has cooled to

$14^{\circ}\text{C}$ . The air temperature increases with increasing height, establishing a warm pool of air over the cool sea surface thereby producing the MAIL. The thickness of the MAIL is less than 160 m (see Figure 5). Maximum cooling of air can occur over the area of the lowest sea surface temperature of  $10^{\circ}\text{C}$  and the relative humidity over this cool area of sea water has a very strong gradient, reaching a value of 92% where fog subsequently forms over the Yellow Sea and adjacent coastal areas including Incheon city ('In' in Figure 6b). Closer to the coast, the SST increases to  $14^{\circ}\text{C}$ , the air cools less and the relative humidity is also lower. At 0600 LST Incheon city reports fog with a relative humidity value of 90–92%.

At approximately 25–50 km offshore (designated by 'Sea' in Figure 6b) and east of Incheon city, the fog is more likely to be denser since, with relative humidity of 92%, the SST there is  $10^{\circ}\text{C}$ , compared to  $14^{\circ}\text{C}$  at the coast. Thus, air parcels over the sea surface with lower SSTs 25–50 km offshore should be much cooler than air with a higher temperature at the coast, and combined with the slightly higher relative humidity, can be expected to lead to the formation of denser fog. At 0600 LST cloud was reported at a height of about 1000 m above the sea and about 30 km offshore from Incheon city but no fog formed over the inland basin containing Seoul city. On the top of Mt Yongmoon, the presence of low cloud is also detected.

#### 4.2. Non-fog formation (day-time)

With a high pressure centre located over the northern part of the Korean peninsula at 0600 UTC, 20 May (1500 LST) and 1200 UTC (2100 LST), the synoptic-scale wind over the centre of the Yellow Sea forms a clockwise circulation, turning from southeasterly, through southerly to southwesterly and northerly during the day. This produces a diffluent wind field (Figures 9a and 9b). Sea fog occurs over the central part of the Yellow Sea but no detailed observations are available at that time (Figures 8a and 8b). Under the influence of the high pressure system over the northern part of the Korean peninsula at 1200 LST 20 May, a diffluent, synoptic-scale westerly wind over the centre of the Yellow Sea combines with a mesoscale westerly sea breeze during daylight hours and becomes a relatively strong onshore wind over the western coast of the Korean peninsula (Figures 9a, 9b, 10a and 10b).

Even though moisture advection occurs over the coast and upslope, condensation into fog does not take place over the coast and inland plain. As the air temperature near the ground increases, the saturation vapour pressure also increases. With the development of a convective boundary layer (CBL), most of the water vapour near the ground is evaporated and rises to the top of the boundary layer, where the temperature of an air parcel is the same as the environment temperature.

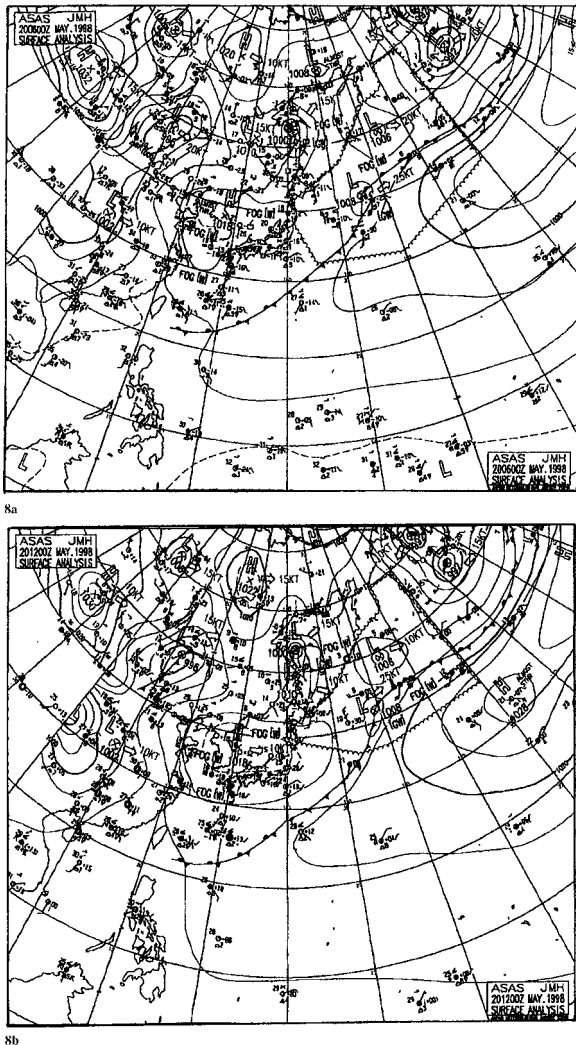


**Figure 8.** (a) MSLP chart at 0600 UTC, 20 May 1998 (1500 LST, 20 May); and (b) as for (a) except at 1200 UTC (2100 LST). At 1200 UTC the high centre is still located over the northern part of the Korean peninsula and the synoptic southwesterly wind prevails near Incheon city. Also, fog is still present over the central part of the Yellow Sea. No information on coastal fog was reported from observations.

Much more water vapour needs to be supplied to the coastal inland basin for condensation to occur.

As shown by the vertical distribution of turbulent diffusion coefficient and sensible heat flux, due to thermal convection the CBL is strongly developed from the coast to further inland and sensible heat flux convergence, implying the heating of air in the boundary layer, takes place close to the land surface (Figures 11a and 11b), resulting in the distribution of high air temperatures at the coast and further inland (Figure 12a). The development of the CBL over the coast can aid in decreasing the water vapour that is transported from the sea and hence there is a lack of fog development over the coast and mountain areas (Figure 12b). The air temperature changes significantly from the coast to the inland basin, but not over the sea surface (Figure 12a). This means that the air at 14 °C

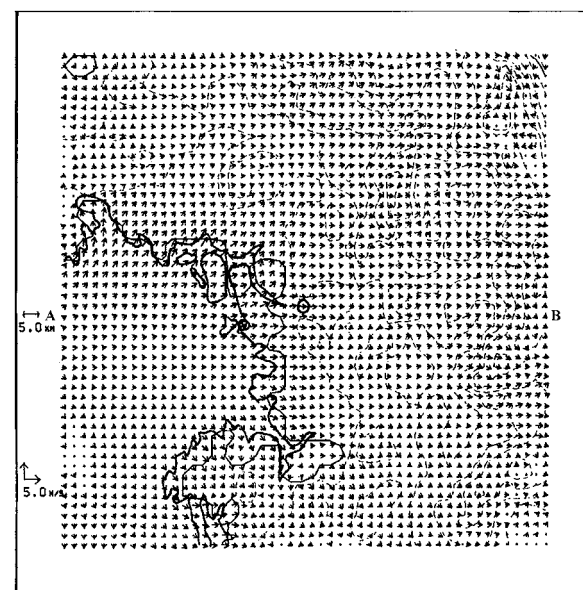
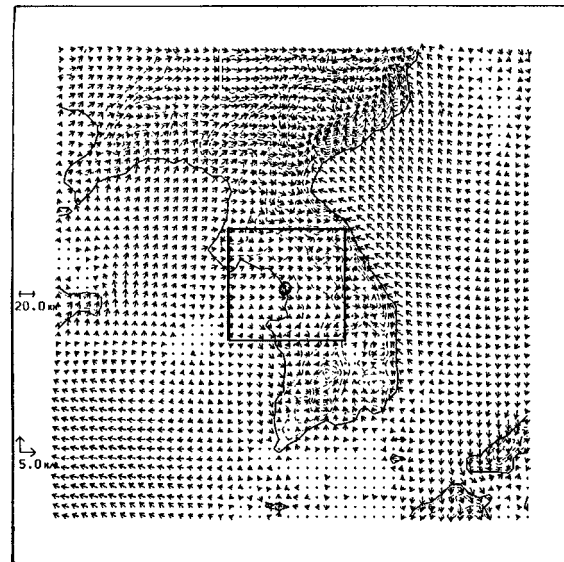


**Figure 9.** (a) Wind vector field ( $m s^{-1}$ ) at 1200 LST, 20 May, 1998 (+24 h) in the coarse-mesh domain near the Korean peninsula; and (b), as for (a), except for the fine-mesh domain near Incheon city. The inset, small circle (left), small circle (centre) and lines (dashed) denote the fine-mesh domain, Incheon city, Seoul city and topographical contours, respectively. A diffluent, synoptic-scale westerly wind over the central part of the Yellow Sea, combined with a westerly sea breeze over the coast, results in a moderate westerly wind near the Incheon coastal area.

above the sea surface retains high relative humidity by being cooled by SSTs as low as 10 °C. The possibility of sea fog formation exists at a distance of 50 km from the coast. However, here the focus is only on the numerical study and verifying observations in order to investigate the formation of coastal fog. At 1200 LST, Incheon Meteorological Observatory reported no fog and a relative humidity of 75%, compared to the model relative humidity of 76%. Similarly at 1200 LST and 1800 LST, a high pressure system is still located over the

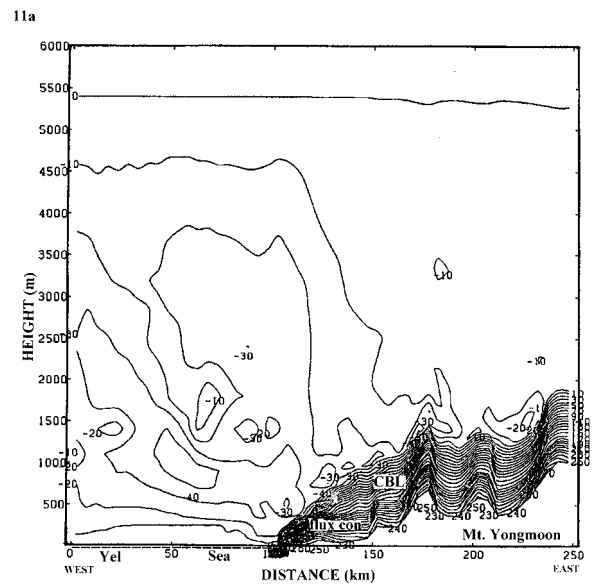
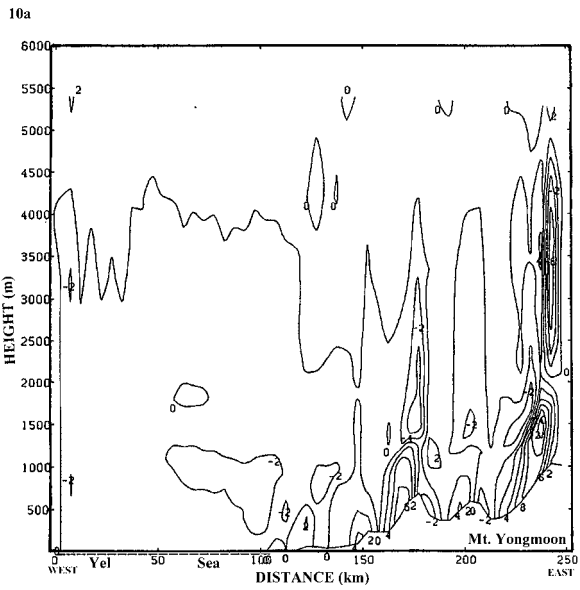
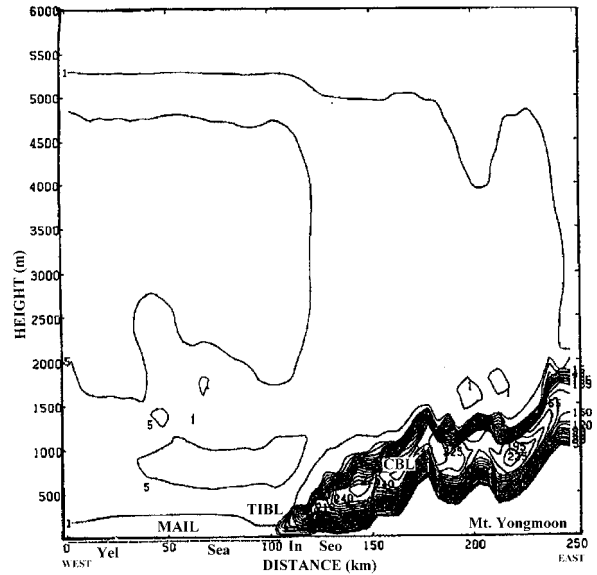
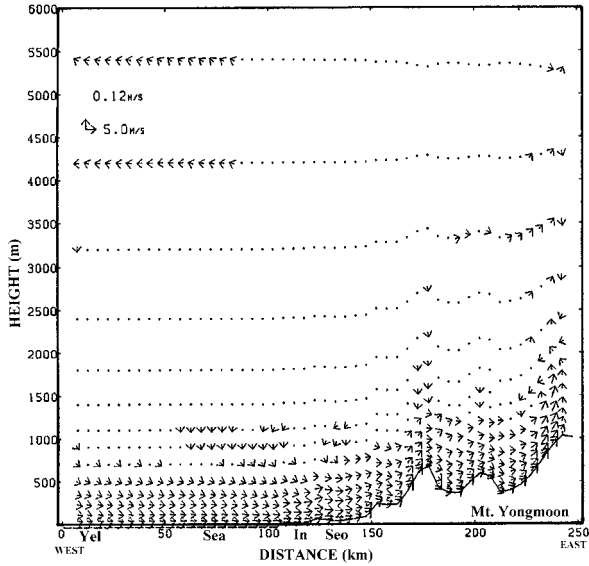


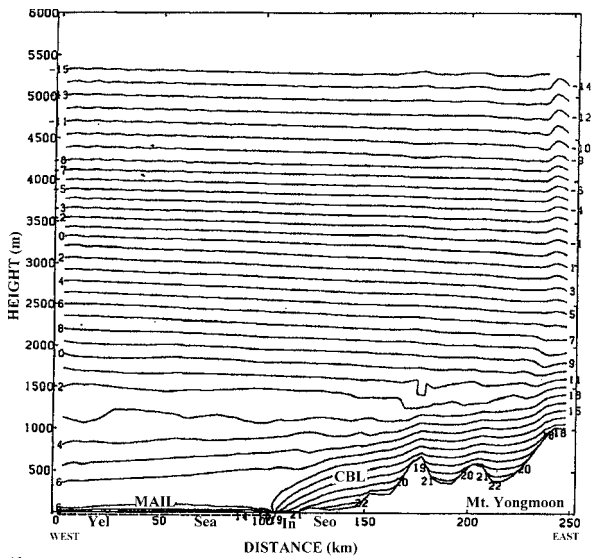
**Figure 10.** (a) Vertical wind profile ( $m s^{-1}$ ; horizontal scale and  $cm s^{-1}$ ; vertical scale) at 1200 LST 20 May on a line AB in Figure 9b; and (b) as for (a) except for vertical wind speed ( $cm s^{-1}$ ). A synoptic-scale westerly wind over the Yellow Sea is enhanced by a sea breeze and valley breeze directed towards the mountains, resulting in a moderate westerly wind near Incheon (In) and a relatively stronger wind near Seoul (Seo). Negative values imply downward vertical motion.

**Figure 11.** (a) As for Figure 10a, except for vertical diffusion coefficient of turbulent heat ( $m^2 s^{-1}$ ); and (b) as for (a) except for sensible heat flux ( $W m^{-2}$ ). MAIL, TIBL and CBL denote marine atmospheric inversion layer, thermal internal boundary layer and convective boundary layer, respectively. The TIBL is developed from the coast near Incheon further inland and the CBL reaches about 800 m in thickness over the surface of the inland basin (Seo) and the mountains further east. 'Flux con' denotes convergence of sensible heat flux, which results in the heating of air above the land surface and the thickening of the CBL.

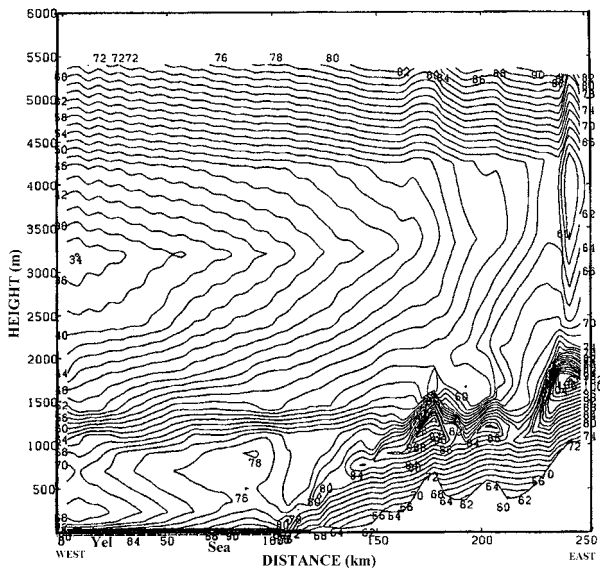
northern part of Korean peninsula near Vladivostok, Russia and a synoptic-scale westerly wind is directed from the Yellow Sea over the coast towards Incheon (not shown). Diurnal thermal heating of the land surface produces a CBL extending from the coast towards the inland basin and along the mountain slope, and at 1800 LST it is slightly thinner in depth compared to 1200 LST (Figures 13a, 13b and 14a). With the decrease in solar radiation at the land surface approaching sunset, the CBL decreases to a depth of about 300 m, just before sunset.

Sensible heat flux convergence is still evident over the land surface at the coast and inland plain, which

maintains the heating of air at the ground and hence there is no fog formation near the surface. The relative humidity is 58% at Incheon city on the coast, but the model result indicates a value of about 70% (Figure 14b). This discrepancy in relative humidity is consistent with the difference in thermal properties between soil and asphalt. Hard road surfaces, typically consisting of asphalt and concrete that retain heat longer than natural surfaces, dominate large cities such as Incheon. Moreover, on roads, moisture can evaporate more



12a



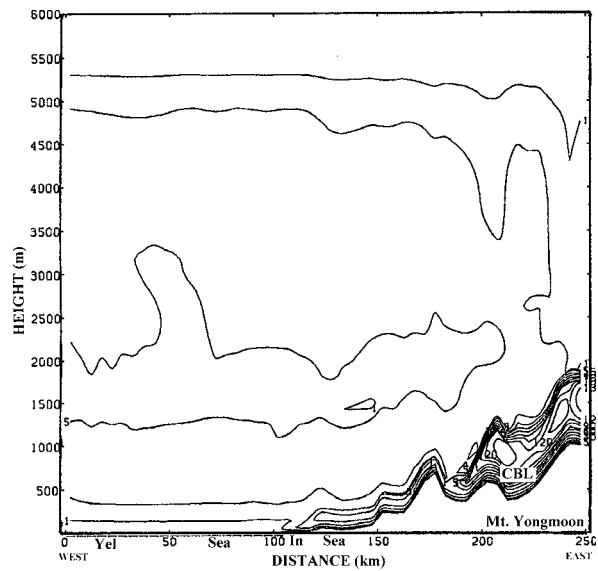
12b

**Figure 12.** (a) As for Figure 10a, except for air temperature ( $^{\circ}\text{C}$ ); and (b), as for (a), except for relative humidity (%) over the Yellow Sea, sea adjacent to the coast and inland plain. Relative humidity about 25–50 km offshore is still high, because air at  $14^{\circ}\text{C}$  over SSTs of  $10^{\circ}\text{C}$  should cool further, enhancing sea fog formation. However, with no difference between air and SSTs at the coast, and with thermal heating of the air over the surface of the inland plain, fog does not form.

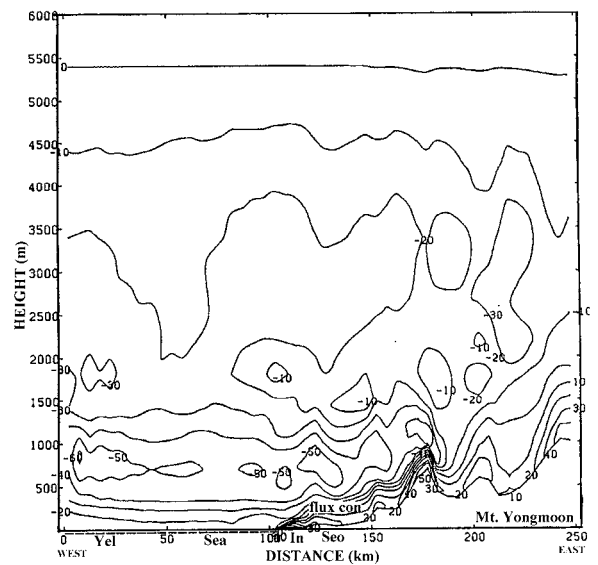
readily thereby reducing the relative humidity at the surface. It is often found that daytime relative humidity is much lower in Incheon city than on its outskirts (KMA 1998). However, these effects were not modelled in this study.

#### 4.3. Fog formation (night and early morning)

On the other hand, at midnight (0000 LST) on 21 May, the synoptic-scale westerly wind affecting the area near Incheon city under the influence of the high pressure system centred over the Yellow Sea, is met by an offshore easterly wind resulting from the combined effect of



13a



13b

**Figure 13.** (a) Profile of vertical diffusion coefficient of turbulent heat ( $\text{m}^2 \text{s}^{-1}$ ) at 1800 LST, 20 May, 1998 (+30 h) on a line AB, as in Figure 9b (Yellow Sea–Incheon–Mt Yongmoon); and (b), as for (a), except for sensible heat flux ( $\text{W m}^{-2}$ ). CBL denotes convective boundary layer. Its depth is approximately 300 m just before sunset near Incheon (In) and Seoul (Seo). ‘Flux con’ denotes convergence of sensible heat flux, which results in heated air just above the land surface, but sensible heat flux decreases due to the decrease in solar radiation around sunset.

an easterly land breeze and mountain katabatic wind affecting the coastal area (not shown). So the nocturnal easterly wind directly opposes the diurnal westerly wind.

At this time, sea fog is reported in the central part of the Yellow Sea on the SLP chart. At Incheon city in the western coastal region of Korea, the model relative humidity value is 80% and Incheon Meteorological Observatory reported fog with a relative humidity of 79%. The driving mechanism for the formation of coastal fog at this time is similar to that for 0600

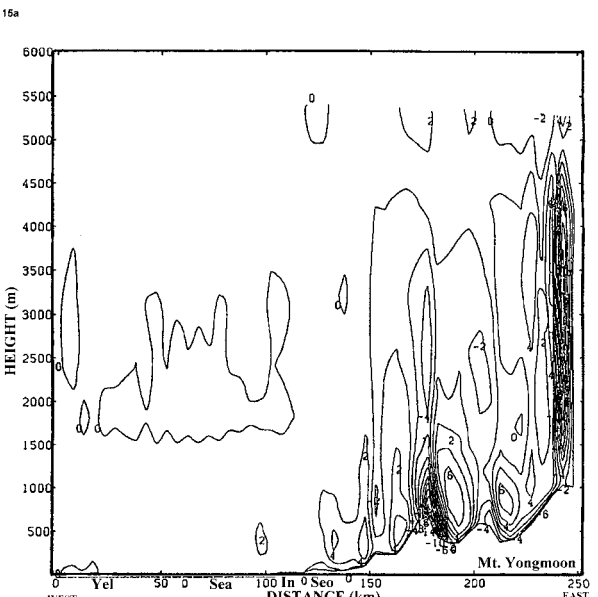
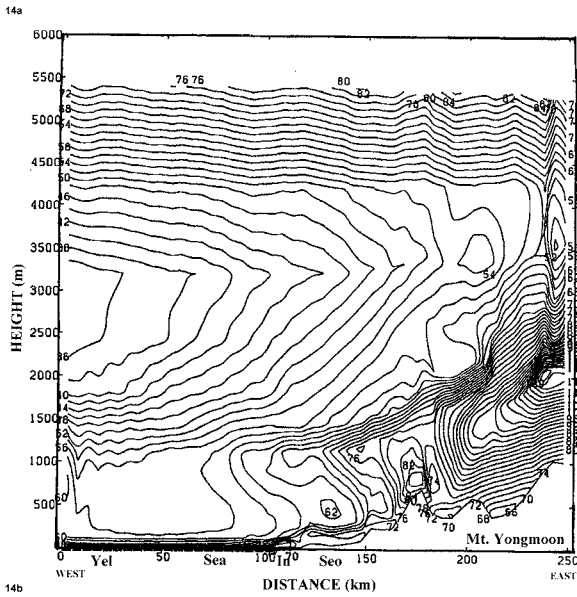
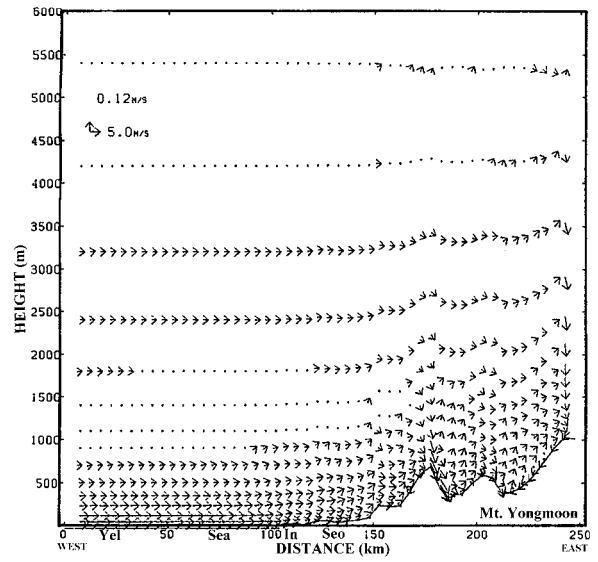
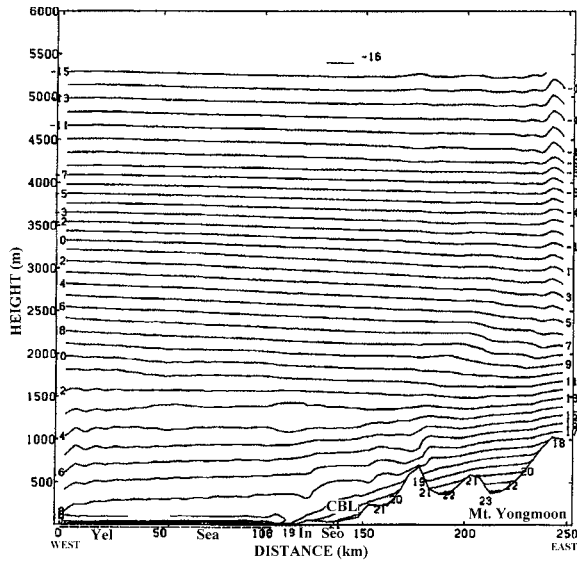


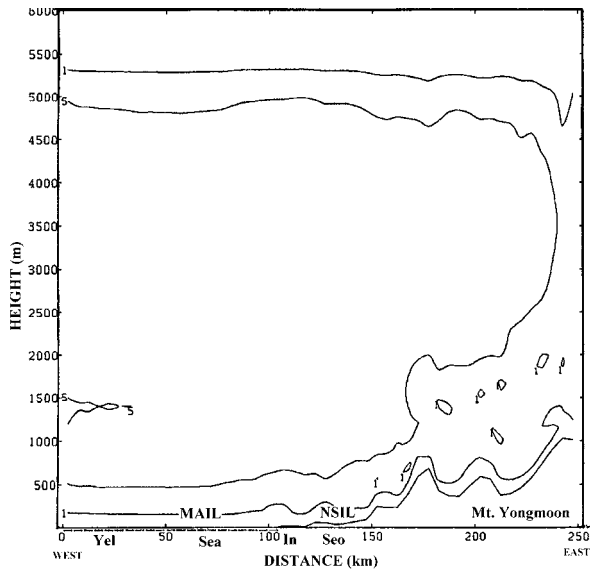
**Figure 14.** (a) As for Figure 13a, except for air temperature ( $^{\circ}\text{C}$ ) over the Yellow Sea denoted by 'Yel', sea adjacent to the coast denoted by 'Sea' and inland (In, Seo); and (b) as for (a) except for relative humidity (%). MAIL and CBL denote marine atmospheric inversion layer and convective boundary layer. Relative humidity over the Yellow Sea is still high, but fog does not form, due to persistent thermal heating of the coastal land surface along the coast. Super-saturation takes place and cloud forms near the top of Mt Yongmoon in the high mountain region.

**Figure 15.** (a) Vertical wind profile ( $\text{m s}^{-1}$ ; horizontal scale and  $\text{cm s}^{-1}$ ; vertical scale) at 0000 LST, May 21, 1998 on a line AB (Yellow Sea–Inchon–Mt Yongmoon), as in Figure 9b; and (b) as for (a) except for vertical wind speed ( $\text{cm s}^{-1}$ ). The synoptic-scale westerly wind suppresses the offshore easterly combined land–mountain breeze, resulting in a moderate westerly wind at the coast near Inchon and Seoul city. 'Yel', 'Sea', 'In' and 'Seo' denote the Yellow Sea, sea adjacent to the coast, Inchon and Seoul cities, respectively. Negative values imply downward vertical motion.

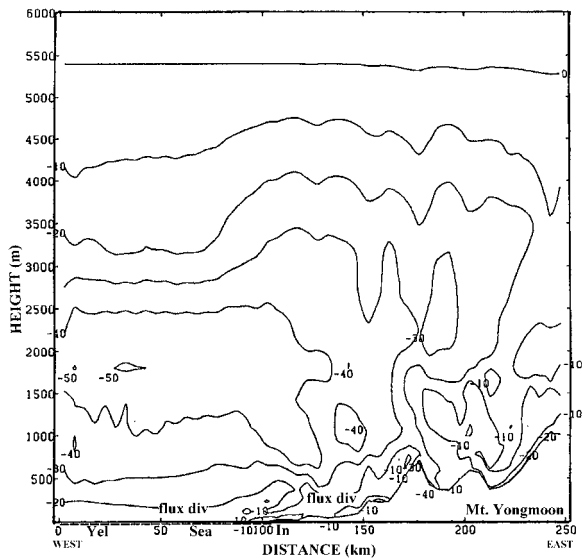
LST, 19 May. As shown in Figures 15a and 15b, the synoptic-scale westerly wind meets an offshore easterly wind. The synoptic-scale westerly wind suppresses the offshore wind, resulting in a moderate westerly wind in the coastal region. Under this scenario, some moisture should be advected from the sea over the inland plain. As shown in Figures 16a, 16b and 17a, sensible heat flux divergence occurs, which is due to nocturnal cooling over the coastal plain and the cooling of air to  $14^{\circ}\text{C}$  over SSTs as low as  $10^{\circ}\text{C}$  offshore. This sensible heat flux divergence can produce an NSIL over the land and an MAIL over the sea surface. From the coast

towards the Yellow Sea, the relative humidity gradient is very strong and at Inchon the relative humidity reaches 89% compared to the model produced value of 86%, indicating the likely formation of coastal fog. However, offshore no fog would be expected with a relative humidity value of 76% in that area. (Figure 17b).

Furthermore, at 0600 LST, the synoptic-scale westerly wind is still evident near the coast, even though diffu-  
 fluence in the wind field is evident over the southeastern



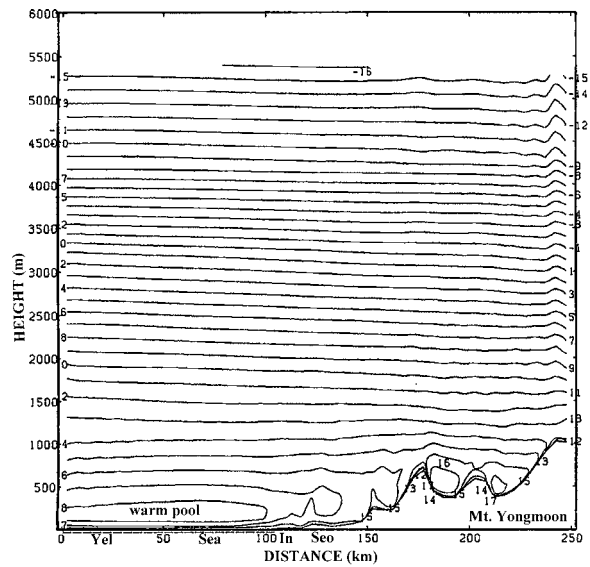
16a



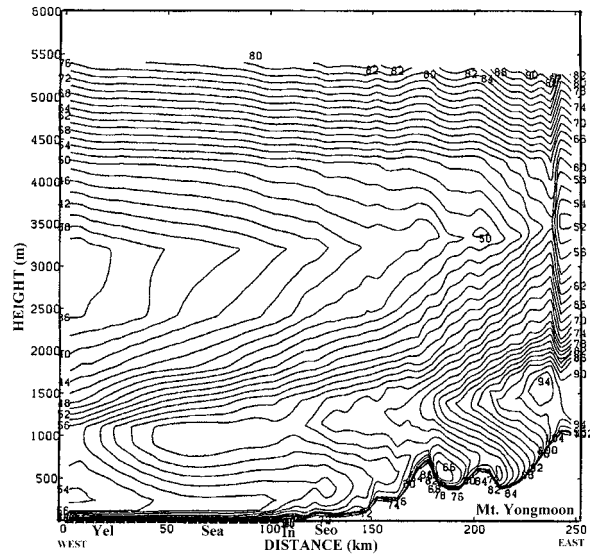
16b

**Figure 16.** (a) As for Figure 15a, except for profile of vertical diffusion coefficient of turbulent heat ( $m^2 s^{-1}$ ); and (b) as for (a) except for sensible heat flux ( $W m^{-2}$ ). MAIL denotes marine atmospheric inversion layer over the Yellow Sea, due to higher air temperature ( $14^\circ C$ ) over the cooler sea surface ( $10^\circ C$ ). NSIL denotes nocturnal surface inversion layer due to cooling over the land surface. 'Flux div' denotes divergence of sensible heat flux, resulting in cooling of air mass over the surface and subsequent fog formation over the sea adjacent to the coast near Incheon city.

part of the Yellow Sea near the southwest coast of Korea (Figures 18a and b). The wind at 0600 LST is much weaker than at 0000 LST. This weak westerly wind could transport moisture inland from the Yellow Sea (not shown). As shown in Figures 19a, 19b and 20a, sensible heat flux divergence occurs over the coastal plain into the lower troposphere. This induces a NSIL inland and a MAIL over the sea surface, characterised by a warm pool of air. Nocturnal cooling of the land and sea surfaces can cause saturation of moist air to thereby produce coastal fog. The observed relative



17a



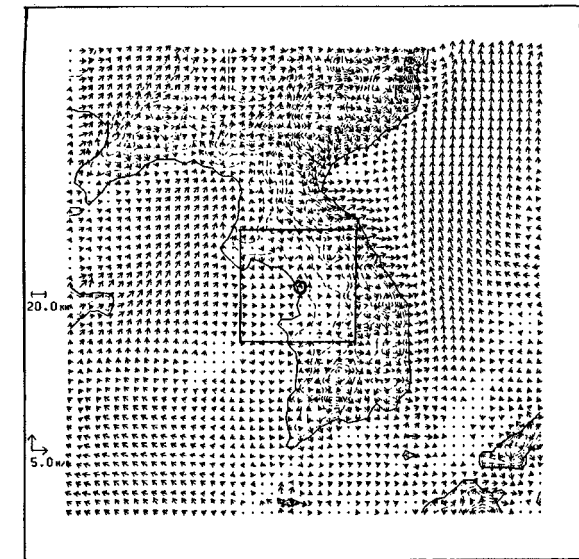
17b

**Figure 17.** (a) As for Figure 15a, except for vertical air temperature profile ( $^\circ C$ ) over the Yellow sea (Yel), sea adjacent to the coast (Sea) and inland (In, Seo); and (b) as for (a) except for relative humidity (%). Relative humidity (%) reaches 80% near the Incheon coast (observed value of 79%) and results in advection fog.

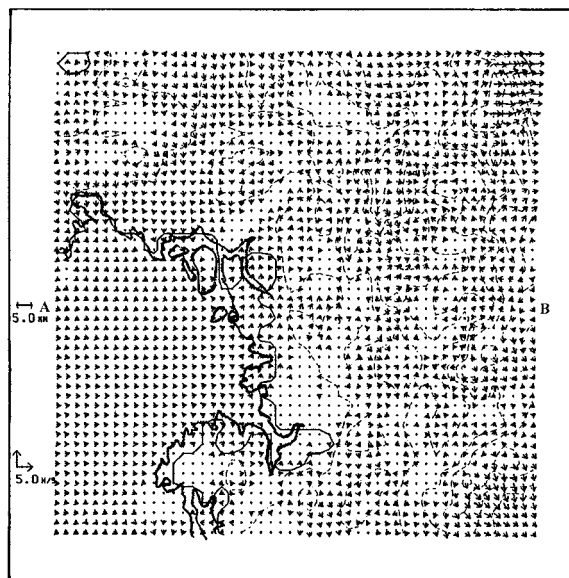
humidity of 89% near the Incheon coast closely matches the model value of 86% in that area (Figure 20b).

#### 4.4. Comparison of model results with observations

The comparison of model predicted and observed relative humidity at Incheon Coastal Meteorological Observatory, which is the closest point to the Yellow Sea coast in the central part of Korean peninsula, is shown in Table 1. The model predicted values closely match the observed values, except at 1800 LST. This discrepancy between model predicted and observed



18a

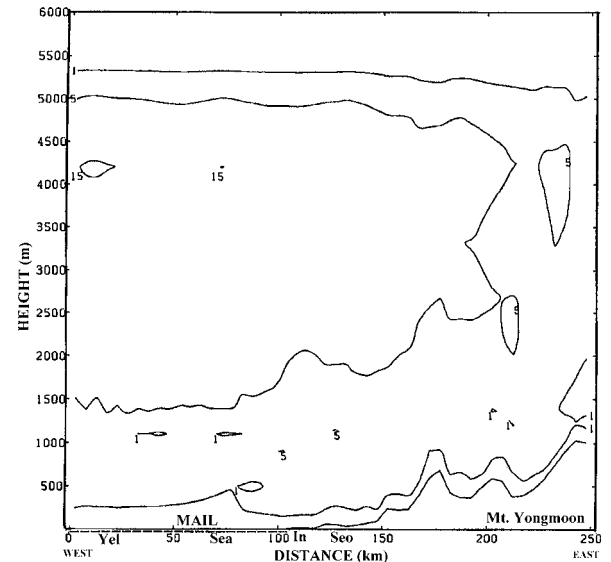


18b

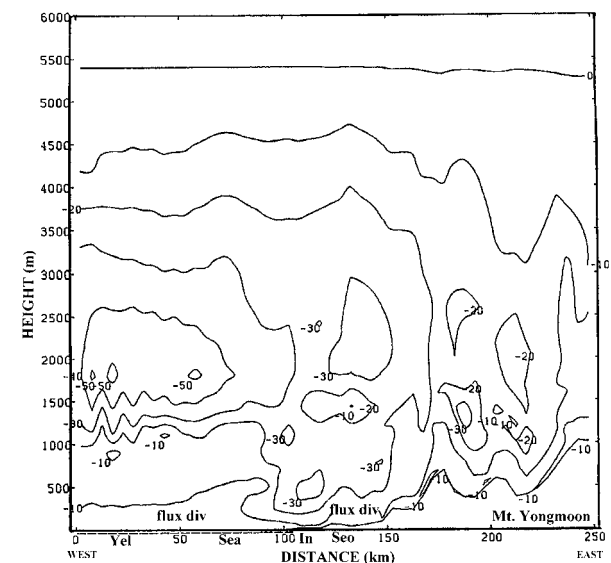
**Figure 18.** Wind vector field ( $m s^{-1}$ ) at 0600 LST, 21 May, 1998 (+42 h). (a) the coarse-mesh domain near the Korean peninsula; and (b) as for (a) except for the fine-mesh domain near Incheon city. The inset, small circle and lines (dashed) denote the fine-mesh domain, Incheon city and topographical contours respectively. The synoptic westerly wind confronts an offshore easterly combined land-katabatic wind, resulting in a moderated westerly wind near the Incheon coast.

Table 1. Comparison of model predicted relative humidity (%) with observed values, 20–21 May 1998, at Incheon Meteorological Observatory, Korea

Day/time	Model predicted rel. humidity (%)	Observed rel. humidity (%)
20 May, 0600 LST	92	96
20 May, 1200 LST	76	75
20 May, 1800 LST	70	58
21 May, 0000 LST	80	79
21 May, 0600 LST	86	89



19a



19b

**Figure 19.** (a) As for Figure 18, except for profile of vertical diffusion coefficient of turbulent heat ( $m^2 s^{-1}$ ) on a line AB as in Figure 15a; and (b), as for (a), except for sensible heat flux ( $W m^{-2}$ ). MAIL denotes marine atmospheric inversion layer evident over in the Yellow Sea, due to higher air temperature ( $14^\circ C$ ) than SST ( $10^\circ C$ ). 'Flux div' denotes sensible heat flux divergence over the sea and land surfaces, which results in cooling of air over the surface and fog formation over the sea adjacent to the coast near Incheon city.

values is possibly due to the greater thermal retention of asphalt than natural surfaces such as soil in the city. In the model, only the effects of properties relating to natural vegetation and soil were considered. However, Incheon Coastal Meteorological Observatory is located close to the centre of Incheon city and it is possible that the lower relative humidity of 58% at this time may be the result of the 'heat island' effect. The focus of this study is on the driving mechanism for fog formation. However, the 'heat island' effect will be investigated in future research.

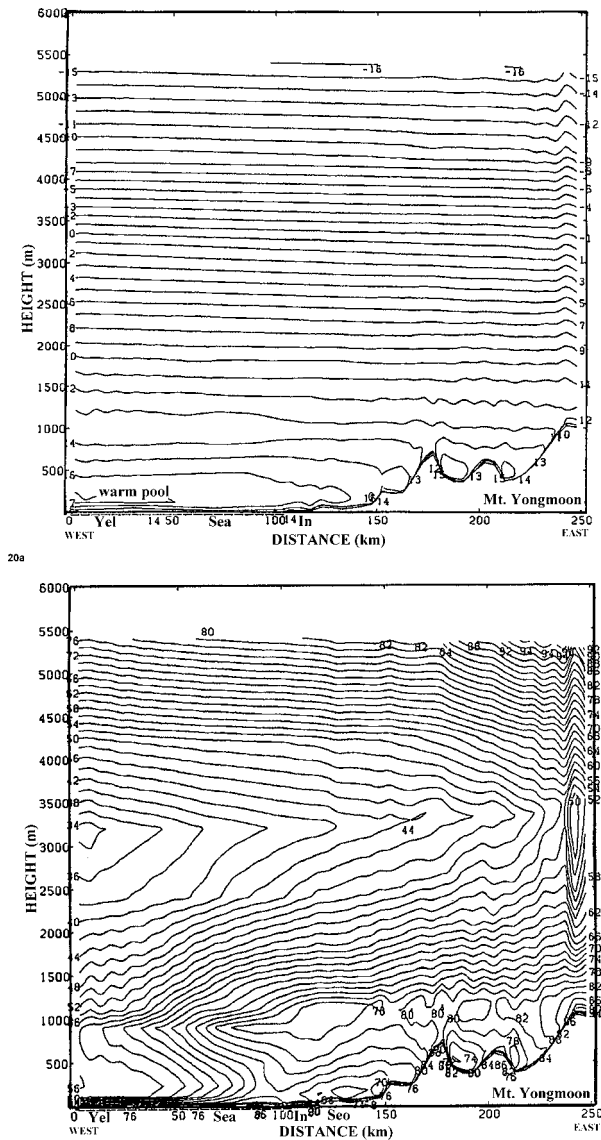


Figure 20. (a) As for Figure 19a, except for vertical air temperature ( $^{\circ}\text{C}$ ); and (b), as for (a), except for relative humidity (%). A warm pool of air forms over the Yellow Sea due to the higher air temperature over the cooler sea surface. The observed relative humidity is 89% near Incheon compared to the model value of 86%, and relative humidity increases from the Yellow Sea over the sea adjacent to the coast ('Sea'), where advection fog forms.

## 5. Conclusions

When high pressure is located near the Korean peninsula, a diffluent wind regime generally occurs over the Yellow Sea, which induces a synoptic-scale southwesterly wind to be directed from the sea towards the Korean peninsula. The synoptic-scale wind near the coast is modified inland by the presence of the local mesoscale effects of the sea breeze, valley wind and mountain katabatic wind. At night or in the early morning, a diffluent westerly wind over the sea extends towards the coast near Incheon city where it meets an easterly offshore wind consisting of a combined land and katabatic mountain breeze. This results in a calm

zone grading to a moderate westerly wind regime near the coast. After sunset, radiational cooling and the intrusion of the westerly wind from the Yellow Sea over the coast can cause moist air to condense, resulting in the formation of advection fog over the coast.

On the other hand, during the day, the synoptic-scale westerly wind is enhanced by a westerly sea breeze and is further intensified by a valley wind directed upslope from the inland basin. Although the resultant strong onshore wind could advect a significant amount of moisture from the sea over the coast, it is very difficult for fog to form because the daytime thermal heating of the land surface can contribute greatly to the development of a thermal internal boundary layer near the coast and a CBL over the coastal plain. This CBL formation has the effect of reducing relative humidity over the inland plain making it difficult for fog to form there.

It is interesting that when an area of sea water with SST as low as  $10^{\circ}\text{C}$  exists offshore and the SST increases toward the coast, as in this case study, air parcels over the cool sea surface can cool further and become saturated, resulting in the formation of sea fog. However, at the coast, nocturnal cooling of the land surface decreases the temperature of the advected moist air driven by the westerly wind, thereby inducing the formation of advection fog over the inland coastal area.

In the past, techniques for forecasting fog in Korea and elsewhere have been mostly limited to an assessment of large-scale meteorological variables for forecasting fog over very small areas with data-sparse observations. The results of this study are encouraging for the further development of fog forecasting with parameters derived from mesoscale model predictions of variables such as relative humidity, temperature and mesoscale circulations that might indicate the likely occurrence of fog. Furthermore, work to improve fog forecasting, for example by high resolution data assimilation into mesoscale numerical weather prediction models and to validate their results, is continuing in most National Weather Centres including KMA, with applications that automatically process night-time NOAA Advanced Very High Resolution Radiometer (AVHRR) multi-spectral satellite data.

## Acknowledgements

The authors wish to thank Mr Syunji Takahashi of the Japan Meteorological Agency for his helpful comments and Dr Junji Sato of the Meteorological Research Institute, Japan for use of the Hitachi supercomputer facility. This work was funded by the Korea Meteorological Administration Research and Development Program under Grant CATER 2006-2-3-9.

## References

- Ahn, J. B., Nam, J. C., Seo, J. W. & Lee, H. J. (2002) Development of sea fog forecasting module and its application to Ulung-island sea fog events. *J. Korean Meteorol. Soc.* **38**: 155–164.
- Businger, J. A. (1973) Turbulence transfer in the atmospheric surface layer. In: D. A. Haugen (ed.), *Workshop on Micrometeorology*, American Meteorological Society, 67–100.
- Choi, H. (1996) Numerical modelling for air flows in the eastern mountainous coastal seas of Korea. *La Mer* **34**: 133–148.
- Choi, H., Kim, J. W. & Takahashi, S. (1998) Three-dimensional numerical prediction of fog formation over coastal complex terrain. *J. Korean Meteorol. Soc.* **34**: 319–335.
- Choi, H., Seo, J. W. & Kim, C. S. (2000) Numerical prediction on sea surface drift induced by windstorm in the coastal complex terrain. *Korean J. Atmos. Sci.* **3**: 67–82.
- Choi, H., Zhang, Y. H. & Takahashi, S. (2004) Recycling of suspended particulates by the interaction of sea-land breeze circulation and complex coastal terrain. *Meteorol. Atmos. Phys.* **87**: 109–120.
- Deardorff, J. W. (1978) Efficient prediction of ground surface temperature and moisture with inclusion of a layer of vegetation. *J. Geophys. Res.* **38**: 659–661.
- Katayama, A. (1972) A simplified scheme for computing radiative transfer in the troposphere. *Technical Report No. 6*, Department of Meteorology, University of California at Los Angeles. 77 pp.
- Kimura, F. & Arakawa, S. (1983) A numerical experiment of the nocturnal low level jet over the Kanto plain. *J. Meteorol. Soc.* **61**: 848–861.
- Kimura, F. & Takahashi, S. (1991) The effects of land-use and anthropogenic heating on the surface temperature in the Tokyo metropolitan area: numerical experiment. *Atmos. Environ.* **25**: 155–164.
- Klemp, J. B. and Durran, D. R. (1983) An upper condition permitting internal gravity wave radiation in numerical mesoscale models. *Mon. Wea. Rev.* **111**: 430–440.
- KMA (1997) *Report of Sea Fog Characteristics in the Coast of Korean Peninsula*. Korean Meteorological Administration, 136 pp.
- KMA (1998) *Daily Meteorological Statistics Data: May 1 through 31, 1998*. Korean Meteorological Administration.
- Lee, Y. H., Kim, D. K. & Min, K. (2000) The role of turbulence in numerical model of sea fog over the Yellow Sea. *J. Korean Meteorol. Soc.* **36**: 643–654.
- Monin, A. S. (1970) The atmospheric boundary layer. *Ann. Rev. Fluid Mech.* **2**: 225–250.
- NFRDA (1998) Analyzed NOAA satellite picture on the sea surface temperature in the East Sea (Japan Sea). *Annual Report 1998*, National Fisheries Research and Development Agency of Korea, 130 pp.
- Orlanski, I. (1976) A simple boundary condition for unbounded hyperbolic flows. *J. Comput. Physics* **21**: 251–269.
- Raynor, G. S., Sethu Raman, S. & Brown, R. M. (1979) Formation and characteristics of coastal internal boundary layer during onshore flows. *Boundary-Layer Meteorol.* **16**: 4587–514.
- Sciocatti, B. (1984) The effect of sea surface temperature on the formation or dispersal of advection fog with the passage of a coastal low. *Proc. Coastal Low Workshop*, Simonstown, 51–52.
- Takahashi, S. (1998) Manual of Las-V model developed by Dr. Junji Sato, Meteorological Research Institute, Japan Meteorological Agency, 30 pp.
- Whiteman, C. D. (1990) Observations of thermally developed wind system in mountainous terrain: atmospheric processes over complex terrain. *Meteorol. Monograph* **40**: 5–42, American Meteorological Society.
- Won, D. J. (2000) Analysis of meteorological and oceanographical characteristics of sea fog over the Yellow Sea. *J. Korean Meteorol. Soc.* **36**: 631–642.
- Yamada, T. (1983) Simulation of nocturnal drainage flows by a  $q^2$  turbulence closure model. *J. Atmos. Sci.* **40**: 91–106.
- Yamada, T. & Mellor, G. L. (1983) A numerical simulation of the BOMEX data using a turbulence closure model coupled with ensemble cloud relations. *Q.J.R. Meteorol. Soc.* **105**: 95–944.